

## Eigenfunctions of the Orr-Sommerfeld/Squire Operator for Channel Flow

A. Leonard

Graduate Aerospace Laboratories  
 California Institute of Technology  
 Pasadena, CA 91125, USA

### Abstract

The eigenfunctions and eigenvalues of the Orr-Sommerfeld/Squire operator for plane channel flow are determined semi-analytically using the WKB approximation. In this case  $k_{\perp} = \sqrt{k_x^2 + k_z^2}$  serves as the eigenvalue for the homogeneous equations, where  $k_x$  and  $k_z$  are wave numbers in the homogeneous directions parallel to the walls. Then for any given complex wave speed  $c$ , the eigenfunctions form a complete set for solutions as a function of  $y$ , the coordinate normal to the walls. Application is made to solving effectively the initial value problem with examples assuming plane Poiseuille base flow.

### Introduction

Knowledge of the eigenvalues and eigenfunctions of the Orr-Sommerfeld/Squire operator can be used in a variety of applications. They, of course, are quite relevant to the prediction of stability and transition in shear flows [5]. They also could be used to construct the resolvent for turbulent wall-bounded flows [4], revealing the linear modes that are most amplified by the nonlinear terms of the Navier-Stokes equations. To determine these eigenfunctions one typically approximates the differential operators by a spectral expansion resulting in large matrices approximating those operators.

In this paper we determine these eigenfunctions and eigenvalues semi-analytically for plane channel flow using the WKB (Wentzel, Kramers, Brillouin) approximation [1]. The eigenfunctions are given in terms of the Bessel functions  $J_1$  and  $Y_1$  and the Airy functions with the wall-normal coordinate  $y$  as the argument. The parameters are the wave numbers in the homogeneous directions  $k_x$  and  $k_z$ , the Reynolds number  $Re$ , and the wave speed  $c = \omega/k_x$ , where the Laplace transform variable  $s = i\omega$ . In this approach the critical layer  $U(y) = c$  requires special attention, as might be expected, as well as the location of a possible turning point where  $d^2U/dy^2 = k_{\perp}^2(c - U(y))$  where  $k_{\perp}^2 = k_x^2 + k_z^2$ . See, for example, [2] to find earlier applications of the WKB method to the analysis of the Orr-Sommerfeld equation.

For the inviscid case, we find that for all  $c$  in the real interval  $[0, U_{max}]$  there is an infinite sequence of eigenfunctions  $v_j(y, c)$  with eigenvalue  $k_{\perp j}(c)$ . We then show how these solutions may be used to solve the initial value problem.

In the viscous case, we find that the eigenfunctions are composed of solutions that have two types of behavior. One type is a relatively slowly varying function of  $y$ , corresponding to an inviscid solution. The other type of behavior is highly oscillatory, varying as  $[(k_x Re)^{1/3}(y - y_c)]^{3/2}$  away from the critical layer at  $y = y_c$ . Again, these eigenfunctions may be used in a variety of ways. One obvious application is to fix  $k_x$  and  $k_z$  to be real constants and then to vary  $Re$  until  $Im(c) = 0$ , determining the point of marginal stability for that Fourier mode.

Applications are made to plane Poiseuille flow.

### Linearized Navier-Stokes Equations

Consider flow in a plane channel with walls at  $y = \pm\delta$  and periodic boundary conditions in the  $x$  and  $z$  directions. In the following we will be working in Fourier space in the  $x$  and  $z$  directions. The steady mean flow and vorticity are given as

$$\begin{aligned} \mathbf{U} &= (U(y), 0, 0) \\ \boldsymbol{\Omega} &= (0, 0, -dU(y)/dy) \end{aligned} \quad (1)$$

We assume the flow is symmetric, i.e.,  $U(-y) = U(y)$  and that  $dU/dy \leq 0$  for  $y \geq 0$ . The linearized Navier-Stokes equations for  $\mathbf{v}$  and  $\boldsymbol{\omega}_y$ , Laplace transformed in time, are then

$$(U(y) - c)D^2\mathbf{v} - U''(y)\mathbf{v} = \frac{-i\nu}{k_x}D^4\mathbf{v} - \frac{i}{k_x}D^2\mathbf{v}_0 \quad (2)$$

$$(U(y) - c)\boldsymbol{\omega}_y + \frac{k_z}{k_x}U'(y)\mathbf{v} = \frac{-i\nu}{k_x}D^2\boldsymbol{\omega}_y - \frac{i}{k_x}\boldsymbol{\omega}_{y0}, \quad (3)$$

where  $D^2 = d^2/dy^2 - k_{\perp}^2$  and where  $k_{\perp}^2 = k_x^2 + k_z^2$ ,  $c = \omega/k_x$ ,  $s = -i\omega$  is the Laplace transform variable, and  $\mathbf{v}$  is the kinematic viscosity. The initial functions of  $\mathbf{v}$  and  $\boldsymbol{\omega}_y$  in time are  $\mathbf{v}_0$  and  $\boldsymbol{\omega}_{y0}$ , respectively. The other velocity components,  $u$  and  $w$ , are then recoverable from the incompressibility constraint and the expression for  $\boldsymbol{\omega}_y$  in terms of derivatives of  $u$  and  $w$ .

### Analysis of the Inviscid Equations

We consider first the homogeneous inviscid equation for  $\mathbf{v}$ , i.e. (2) with  $\mathbf{v}$  and  $\mathbf{v}_0 = 0$ .

$$\frac{d^2\mathbf{v}}{dy^2} - \left( \frac{U''(y)}{U(y) - c} + k_{\perp}^2 \right) \mathbf{v} = 0. \quad (4)$$

We assume (4) is amenable to a WKB solution

so that  $\mathbf{v}(y)$  is given approximately as

$$\mathbf{v}(y) = \chi^{-1/4}(y) \exp\left(\pm i \int^y \sqrt{\chi(y')} dy'\right), \quad (5)$$

where

$$\chi(y) = -\frac{U''(y)}{U(y) - c} - k_{\perp}^2 \quad (6)$$

The approximation is not valid in the neighborhood of a critical point  $y_c$  where  $U(y_c) = c$  and therefore requires modification. See [3] for details.

### Homogeneous Solutions to the Inviscid Equations

In this section we look for homogeneous solutions to the inviscid form of the Orr-Sommerfeld/Squire equations, i.e., (2)

and (3) with the RHS's set to zero and satisfying the inviscid boundary conditions. Thus we first consider the equation for the eigenfunction  $v_j$  with eigenvalue  $k_{\perp j}$

$$\frac{d^2 v_j}{dy^2} - \frac{U''(y)v_j}{U(y)-c} = k_{\perp j}^2 v_j \quad (7)$$

with  $v_j(\pm\delta, c) = 0$ . We find, with the WKB method discussed in the previous section, in fact, that for each  $c$ , real or complex, there is an infinite sequence of eigenfunctions  $v_j$  each with eigenvalue  $k_{\perp j}$ , ( $j = 0, 1, 2, \dots$ ) with the even indices assigned to the even eigenfunctions ( $v_j(-y) = v_j(y)$ ) and odd indices to the odd eigenfunctions. For  $c \rightarrow c^*$  there are also corresponding complex conjugate solutions  $v_j^*$  with eigenvalue  $k_{\perp j}^*$  obtained by simply taking the conjugate of (7). If  $c$  is real then we take  $(v_j, k_{\perp j})$  as the solution for  $Im(c) \rightarrow 0^+$  and  $(v_j^*, k_{\perp j}^*)$  the solution corresponding to  $Im(c) \rightarrow 0^-$ .

It is easily shown that  $v_j$  is orthogonal to  $v_k$ , i.e.,

$$\int_{-\delta}^{\delta} v_k(y, c) v_j(y, c) dy = C_j \delta_{kj} \quad (8)$$

if  $k_{\perp k}^2 \neq k_{\perp j}^2$ . And, similarly,  $v_j^*$  is orthogonal to  $v_k^*$  for  $j \neq k$ .

In Figure 1 the eigenvalues for the two lowest even modes,  $j = 0$  and  $j = 2$ , are shown as  $c$  varies from 0 to 1 in plane Poiseuille flow,  $U(y) = 1 - y^2$ . Similar plots for the lowest odd modes,  $j = 1$  and  $j = 3$ , are shown in Figure 2.

The first odd eigenfunction for  $c = 0.4$ ,  $v_1(y, 0.4)$ , is shown in Figure 3 and the corresponding second even eigenfunction,  $v_2(y, 0.4)$ , is shown in Figure 4.

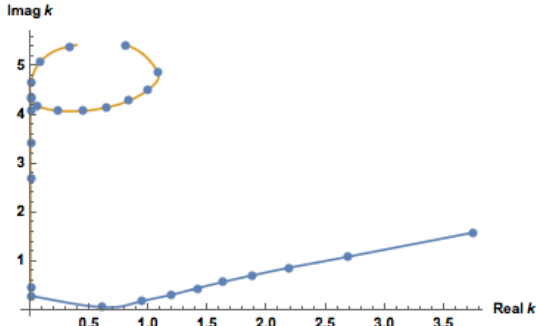


Figure 1: Eigenvalues  $k_{\perp}$  for the two lowest even modes,  $j = 0$  (blue) and  $j = 2$  (yellow) as  $c$  varies from 0 to 1 in plane Poiseuille flow,  $U(y) = 1 - y^2$ . The plots start on the imaginary axis for  $c = 0$ . For the case  $j = 2$  the curve returns to the imaginary axis at  $c \approx 0.95$  after a counterclockwise trajectory.

### Solution to the Initial Value Problem

In this section we use the homogeneous solutions determined above to give an effective solution to the initial value problem, i.e. (5) with  $v = 0$ . As will be shown, this leads to an expansion of  $v(x, y, z, t)$  in terms of the  $v_j(y, c)$  modes traveling with real speed  $c$  that are furthermore localized in  $(x - ct, z)$  in the wall-parallel directions.

Assume, for the moment, that  $Im(c) \neq 0$ . Substituting the expansion

$$v(k_x, y, k_z, c) = \sum_j b_j(k_x, k_z, c) v_j(y, c) \quad (9)$$

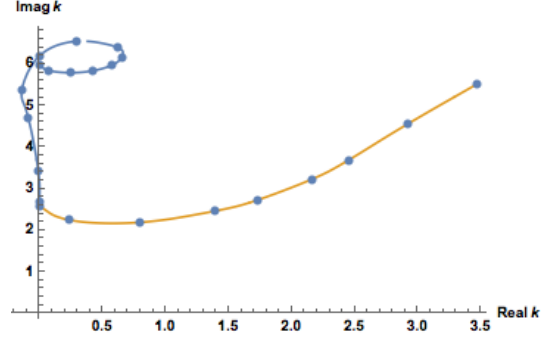


Figure 2: Eigenvalues  $k_{\perp}$  for the two lowest odd modes,  $j = 1$  (yellow) and  $j = 3$  (blue) as  $c$  varies from 0 to 1 in plane Poiseuille flow,  $U(y) = 1 - y^2$ . The plots start on the imaginary axis for  $c = 0$ . For the case  $j = 3$  the curve returns to the imaginary axis at  $c \approx 0.8$  after a counterclockwise trajectory.

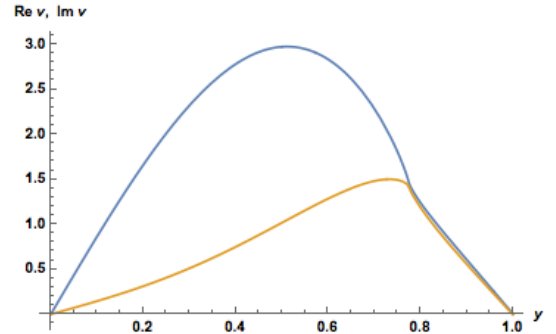


Figure 3: Real (blue) and imaginary (yellow) parts of the first odd eigenfunction for  $c = 0.4$ ,  $v_1(y, 0.4)$ .

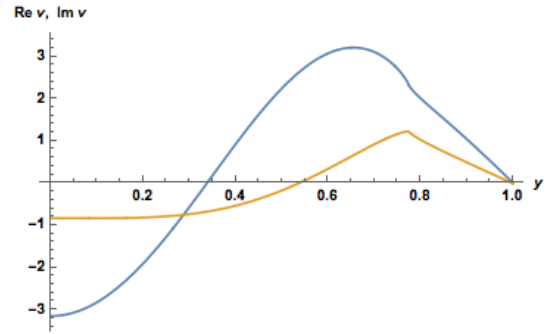


Figure 4: Real (blue) and imaginary (yellow) parts of the second even eigenfunction for  $c = 0.4$ ,  $v_2(y, 0.4)$ .

into the inviscid form of (5) and using (8) with the assumption  $C_j = 1$ , we find that

$$b_j = \frac{-i}{k_x(k_{\perp j}^2(c) - k_{\perp}^2)} \int_{-\delta}^{\delta} \frac{v_j(y', c) \nabla^2 v_0(k_x, y', k_z) dy'}{U(y') - c}. \quad (10)$$

## Laplace Inversion

The inverse Laplace transform is given by

$$\frac{1}{2\pi} \int_{\Gamma_\omega} \mathfrak{v}(k_x, y, k_z, \omega/k_x) e^{-i\omega t} d\omega = \frac{k_x}{2\pi} \int_{\Gamma_c} \mathfrak{v}(k_x, y, k_z, c) e^{-ik_x ct} dc, \quad (11)$$

where we have used  $\omega = k_x c$ .  $\Gamma_\omega$  is the integration path from  $-\infty + ia$  to  $\infty + ia$  with  $a > 0$ , i.e., above all singularities in the complex  $\omega$  plane and therefore the integration path for  $\Gamma_c$  is from  $-sgn(k_x)\infty + ia/k_x$  to  $sgn(k_x)\infty + ia/k_x$ . In addition, it is easily shown that for  $c$  large,  $k_\perp^2(c) \rightarrow -(j+1)\pi/2\delta^2$  and

$$\mathfrak{v}_j(y, c) \rightarrow \cos\left[\frac{(j+1)\pi y}{2\delta}\right], \quad (j = 0, 2, \dots) \quad (12)$$

$$\mathfrak{v}_j(y, c) \rightarrow \sin\left[\frac{(j+1)\pi y}{2\delta}\right], \quad (j = 1, 3, \dots) \quad (13)$$

as  $|c| \rightarrow \infty$ . Thus, except for the factor  $1/(U(y') - c)$  in (10),  $\mathfrak{v}(k_x, y, k_z, c)$  becomes independent of  $c$  as  $|c| \rightarrow \infty$ . For the inviscid case the functions  $\mathfrak{v}_j(y, c)$  contain terms proportional to  $\log(U(y) - c)$ . Thus if we take  $\max_y[U(y)] = 1$  then  $\mathfrak{v}(k_x, y, k_z, c)$  will have a branch cut on the real axis,  $0 \leq c \leq 1$ , with an embedded simple pole at  $c = U(y')$ . The net result is that  $\Gamma_c$ , regardless of  $sgn(k_x)$  can be reduced to a closed contour encircling the branch cut plus pole in the clockwise direction:

$$\mathfrak{v}(k_x, y, k_z, t) = \frac{i}{2\pi} \sum_j \oint \frac{\mathfrak{v}_j(y, c) q_j(k_x, c, k_z)}{(k_\perp^2(c) - k_\perp^2)} e^{-ik_x ct} dc, \quad (14)$$

where

$$q_j(k_x, c, k_z) = \int_0^1 \frac{\mathfrak{v}_j(y_{c'}, c) \nabla^2 \mathfrak{v}_{0\pm}(k_x, y_{c'}, k_z) dc'}{(c - c') U'(y_{c'})} \quad (15)$$

and where we have changed the integration variable  $y'$  to  $c'$  by defining  $U(y') = c'$  and  $y_{c'} = U^{-1}(c')$  and introducing the function  $\nabla^2 \mathfrak{v}_{0\pm}(k_x, y_{c'}, k_z) = \nabla^2 \mathfrak{v}_0(k_x, y_{c'}, k_z) + (-1)^j \nabla^2 \mathfrak{v}_0(k_x, -y_{c'}, k_z)$ .

## Fourier Inversion

From (14,15) we see that to obtain  $\mathfrak{v}(x, y, z, t)$  we will need to perform an inverse transform on the product of  $\nabla^2 \mathfrak{v}_{0\pm}(k_x, y_c, k_z)$  or  $q_j(k_x, c, k_z)$  with  $1/(k_\perp^2 - k_\perp^2_j(c))$ . Thus the result will be the equivalent of the convolution of  $q_j(x, c, z)$  with the inverse transform of  $1/(k_\perp^2 - k_\perp^2_j(c))$  displaced in  $x$  by  $ct$ . For 2D applications (no  $z$  dependence) we find, taking  $Im(k_\perp^2_j) \geq 0$ , that this inverse transform is simply

$$\frac{1}{2\pi} \int_{-\infty}^{\infty} \frac{e^{ik_x x} dk_x}{k_x^2 - k_\perp^2_j(c)} = \frac{i}{2k_\perp^2_j(c)} e^{ik_\perp^2_j(c)|x|} \quad (16)$$

and therefore

$$\mathfrak{v}(x, y, t) = \frac{1}{4\pi} \sum_j \oint \frac{\mathfrak{v}_j(y, c) \left( \int_{-\infty}^{\infty} q_j(x', c) e^{ik_\perp^2_j(c)|x-x'-ct|} dx' \right) dc}{k_\perp^2_j(c)}. \quad (17)$$

Similarly, the inverse transform of  $1/(k_\perp^2 - k_\perp^2_j(c))$  with  $x$  and  $z$  dependence is

$$\frac{1}{4\pi^2} \int_{-\infty}^{\infty} \int_{-\infty}^{\infty} \frac{e^{ik_x x + ik_z z} dk_x dk_z}{(k_\perp^2 - k_\perp^2_j(c))} = \frac{1}{2\pi} K_0(-ik_\perp r), \quad (18)$$

where  $K_0$  is the modified Bessel function and  $r = \sqrt{x^2 + y^2}$ . Therefore

$$\mathfrak{v}(x, y, z, t) = \frac{-i}{4\pi^2} \sum_j \oint \mathfrak{v}_j(y, c) \int_{-\infty}^{\infty} \int_{-\infty}^{\infty} K_0(-ik_\perp \sqrt{(x-ct-x')^2 + (z-z')^2}) q_j(x', c, z') dx' dz' dc. \quad (19)$$

Notice from (16) that the  $(c, j)$  combinations that lead to smaller imaginary parts of  $k_\perp$  will generally yield higher amplitude contributions to  $\mathfrak{v}$  from the initial field  $\mathfrak{v}_0$ . This is true also for the cases of  $(x, z)$  dependence. For the lowest even mode,  $j = 0$ , we found an approximate minimum imaginary part for  $c = 0.1$  with  $k_{\perp 0} = 0.6 + 0.65i$ . Similarly, for  $j = 1$  the minimum occurs at approximately  $c = 0.4$  with  $k_{\perp 1} = 0.795 + 2.19i$ , still a larger imaginary part than that of  $k_{\perp 0}(c)$  for all  $c$ . The corresponding plots for  $\frac{1}{2\pi} K_0(-ik_\perp r)$  are shown in Figure 5. Note the wide difference between the cases  $j = 0$  and  $j = 1$ .

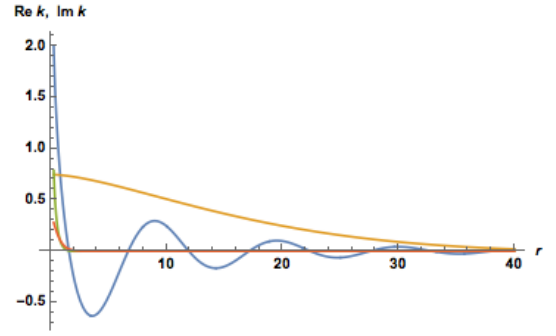


Figure 5: Real (blue) and imaginary parts (yellow) of  $\frac{1}{2\pi} K_0(-ik_\perp r)$  for  $c = 0.1$ ; Real (green) and imaginary parts (red) of  $\frac{1}{2\pi} K_0(-ik_\perp r)$  for  $c = 0.4$ . Not shown for  $r < 0.25$  because of the singularity of  $K_0$  at  $r = 0$ .

## Solutions to the Squire Equation

To complete the analysis of the inviscid form of (3), we can solve the initial value problem for  $\omega_y$  simply as

$$\omega_y = -\frac{k_z}{k_x} \frac{U'(y)}{(U(y) - c)} \mathfrak{v} - \frac{i}{k_x (U(y) - c)} \omega_{y0} + C\delta(U(y) - c), \quad (20)$$

where  $\mathfrak{v}$  is now assumed known and  $C$  depends on  $\omega$ ,  $k_x$ , and  $k_z$ . However a sometimes more useful equation for  $\omega_y$  is given in terms of the original independent variables  $(x, y, z, t)$ :

$$\frac{\partial \omega_y}{\partial t} + U(y) \frac{\partial \omega_y}{\partial x} = -U'(y) \frac{\partial \mathfrak{v}}{\partial z} + \mathfrak{v} \nabla^2 \omega_y. \quad (21)$$

Solving (21) directly with the initial condition  $\omega_y(x, y, z, 0) = \omega_{y0}(x, y, z)$  and  $\mathfrak{v}$  given yields

$$\omega_y(x, y, z, t) = \omega_{y0}(x - U(y)t, y, z) - U'(y) \int_0^t \frac{\partial \mathfrak{v}}{\partial z}(x - U(y)(t - t'), y, z, t') dt'. \quad (22)$$

Note from (22) that  $\omega_y$  is being generated continuously as long as  $\partial v/\partial z \neq 0$ . And it therefore follows from (19) that the function  $\partial K_0(-ik_\perp r)/\partial z$  will play an important role in the generation of  $\omega_y$ . This function is shown in Figures 6 and 7 for the case  $c = 0.1, j = 0$ .

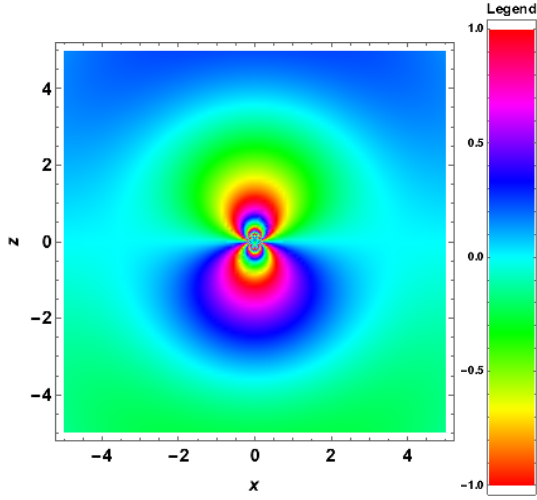


Figure 6: Real part of  $\partial K_0(-ik_\perp r)/\partial z$  for the case  $c = 0.1, j = 0$ .

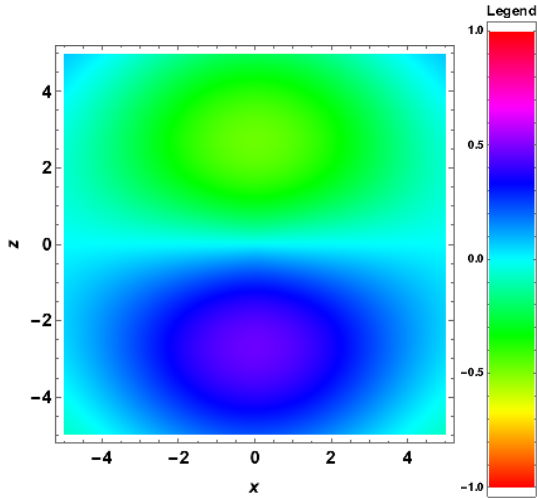


Figure 7: Imaginary part of  $\partial K_0(-ik_\perp r)/\partial z$  for the case  $c = 0.1, j = 0$ .

### Homogeneous Solutions to the Viscous Equations

The homogeneous viscous equation for  $v$  can be rewritten as

$$\begin{aligned} \frac{d^4 v}{dy^4} - iR_k \left( U(y) - c - \frac{2ik_\perp^2}{R_k} \right) \frac{d^2 v}{dy^2} \\ + iR_k \left( U''(y) + k_\perp^2 (U(y) - c) - \frac{ik_\perp^4}{R_k} \right) v = 0, \end{aligned} \quad (23)$$

where  $R_k = v/k_x$ . See Equation (2). Following the WKB method we assume

$$v = \exp(iS(y)) \quad (24)$$

and that  $|S'^2| \gg |S''|$ . Substituting (24) into (23) and assuming  $S = S_0 + S_1 + \dots$ , we find two solutions for  $S_0'^2$ :

$$(S_0'^2)_\pm = -\frac{iR_k}{2} \left( U(y) - c \pm \sqrt{(U(y) - c)^2 + \frac{4iU''(y)}{R_k}} \right) - k_\perp^2, \quad (25)$$

and an equation for the next order term  $S_1'$  in terms of  $S_0'$  and  $S_0''$ . For reference, application of the above procedure applied to the inviscid equation gives  $S_0'^2 = \chi(y)$  given by (6) and  $S_1' = -\frac{S_0''}{2S_0'}$  so that  $S_1 = -\frac{1}{4} \log(\chi(y))$ , as seen in (5).

Examining the result (25), we find that  $(S_0'^2)_+$  asymptotes to the inviscid result (6) as  $y$  increases away from the critical point  $y_c$  ( $U(y_c) = Re(c)$ ). A similar result obtains for  $(S_0'^2)_-$  as  $y$  decreases away from  $y_c$ . On their respective opposites sides of  $y_c$  the analysis leads to highly oscillatory behavior for  $v \sim [(k_x Re)^{1/3} (y - y_c)]^{3/2}$  away from the critical point. Finally, the approximation  $S \approx S_0 + S_1$  is not valid for  $y$  in the neighborhood of  $y_c$ . The above solutions must be matched to inner solutions given by modified Airy functions [2] or by solutions obtained by Fourier Transform methods. Then we proceed as in the inviscid case above with three potentially complex parameters  $c, k_x$ , and  $k_\perp$ , for a given Reynolds number  $= 1/\nu$ .

### Summary and Conclusions

The eigenfunctions and eigenvalues of the Orr-Sommerfeld/Squire operator for plane channel flow are determined semi-analytically using the WKB approximation. In this case  $k_\perp$  serves as the eigenvalue for the homogeneous equations. For any given complex wave speed  $c$ , the eigenfunctions form a complete set for solutions as a function of  $y$ , the coordinate normal to the walls. Application is made to solving effectively the initial value problem for inviscid flows with examples assuming plane Poiseuille base flow. Notably, specific ranges of  $c$  for the lower order modes in  $y$  have smaller values of  $Imag(k_\perp)$  yielding particularly important contributions to the solution. This result is apropos to the goal of obtaining reduced-order representations of the flow field as it is for resolvent analysis.

### REFERENCES

1. Bender, C. M. & Orszag, S. A., 1978 *Advanced Mathematical Methods for Scientists and Engineers*, McGraw-Hill.
2. Drazin, P. G. & Reid, W. H., *Hydrodynamic Stability*, Cambridge University Press, 1981.
3. Leonard, A. 2016 Approximate Solutions to the Linearized Navier-Stokes Equations for Incompressible Channel Flow, *Proc. 20th Australasian Fluid Mechanics Conference*.
4. McKeon, B. J. & Sharma, A. S. 2010 A critical-layer framework for turbulent pipe flow, *J. Fluid Mech.* **658**, 336-382.
5. Schmid, P. J. & Henningson D. S. 2001 *Stability and Transition in Shear Flows*, Springer-Verlag.